Available online at www.sciencedirect.com
ScienceDirect
Journal of Power Sources 166 (2007) 35–40
JOURNAL OF POWER SOURCES
www.elsevier.com/locate/jpowsour

Short communication

Preparation and characterization of strontium and magnesium doped lanthanum gallates as the electrolyte for IT-SOFC

Dokyol Lee [a], Ju-Hyeong Han [a,*], Youngsuk Chun [a], Rak-Hyun Song [b], Dong Ryul Shin [b]

[a] *Department of Materials Science and Engineering, Korea University, 5-1 Anam-Dong, Sungbuk-Ku, Seoul 136-701, Republic of Korea*
[b] *Advanced Fuel Cell Research Team, Korea Institute of Energy Research, 71-2 Jang-dong, Yusong-gu, Daejon 305-343, Republic of Korea*

Received 12 November 2006; received in revised form 22 December 2006; accepted 22 December 2006
Available online 17 January 2007

Abstract

LSGM ($La_{1-x}Sr_xGa_{1-y}Mg_yO_{3-\delta}$) powders of four different compositions (x, $y = 0.1$ or 0.2) (a symbolic system such as LSGM9191 for $x = 0.1$ and $y = 0.1$ or LSGM9182 for $x = 0.1$ and $y = 0.2$ is used hereafter) were synthesized using the GNP (glycine nitrate process) as the electrolyte material of the intermediate temperature solid oxide fuel cell (IT-SOFC). They were then calcined at 1000 °C for 2 h, compacted into a disc or a rod, and sintered at 1400 °C for 4 h in preparation for structural, electrical and thermomechanical characterizations. The reactivity of the LSGM with the cathode material of LSM ($La_{0.85}Sr_{0.15}MnO_3$) or with the anode material of Ni–YSZ was analyzed by sintering an LSGM/LSM, LSGM/NiO or LSGM/YSZ powder mixture at 1400 °C for 4 h and then searching for possible reaction products in its XRD pattern. The sinters of LSGM9191, LSGM9182 and LSGM8282 consisted of a single LSGM phase. On the other hand, the sinter of LSGM8291 contained the second phases of $LaSrGa_3O_7$ and $LaSrGaO_4$ as well in addition to the main LSGM phase. The electrical conductivity of LSGM8282 (0.105 S cm^{-1} at 800 °C) turned out to be the highest among those of the four LSGMs and more than twice as high as that of YSZ (~0.045 S cm^{-1}). The linear thermal expansion coefficient was measured to be 12.1×10^{-6} K^{-1} for LSGM8282 which was very close to that of LSM (11.7×10^{-6} K^{-1}). The phase stability of LSGM8282 in contact with LSM was fairly good. LSGM8282, however, reacted quite extensively with Ni–YSZ.

Keywords: SOFC; LSGM; GNP; Electrolyte

1. Introduction

At present, one of the most well-known electrolyte materials for the solid oxide fuel cell (SOFC) is yttria-stabilized zirconia (YSZ). However, the working temperature of YSZ is quite high (~1000 °C), which causes its constituent materials to be oxidized under oxidizing atmosphere. Moreover, this high working temperature limits the components of the cell to expensive ceramic materials. Therefore, the development of intermediate temperature SOFC (IT-SOFC) is the key to their commercialization. Among the many research organizations that have studied ways to lower the temperature of the SOFC, the Korea Institute of Energy Research is developing anode-supported flat-tube cells and stacks operated at intermediate temperatures (≤800 °C) with Ni–YSZ, YSZ and LSM/LSCF as the anode, electrolyte and cathode materials, respectively [1]. In conjunction with this effort, our laboratory is in the process of preparing various superior oxide-ion electrolyte powders such as ScSZ (scandia-stabilized zirconia), LSGM and BiO_2-based ceramics and characterizing them as the alternative possibly replacing the YSZ electrolyte for enhanced cell performance.

In this study, the LSGM powders of various compositions were prepared using GNP, known to produce oxide powders compositionally uniform up to atomic scale and fine enough to be readily sinterable to high densities [2], and the one with maximum electrical conductivity was characterized to see if it could serve as an alternative electrolyte for the IT-SOFC.

2. Experimental procedure

LSGM ($La_{1-x}Sr_xGa_{1-y}Mg_yO_{3-\delta}$) powders of four different compositions (x, $y = 0.1$ or 0.2) were prepared as the electrolyte material for IT-SOFCs. These compositions were chosen because a single LSGM phase could be expected when

* Corresponding author. Tel.: +82 2 3290 3707; fax: +82 2 928 3584.
E-mail address: hanjuh99@korea.ac.kr (J.-H. Han).

0378-7753/$ – see front matter © 2007 Elsevier B.V. All rights reserved.
doi:10.1016/j.jpowsour.2006.12.099

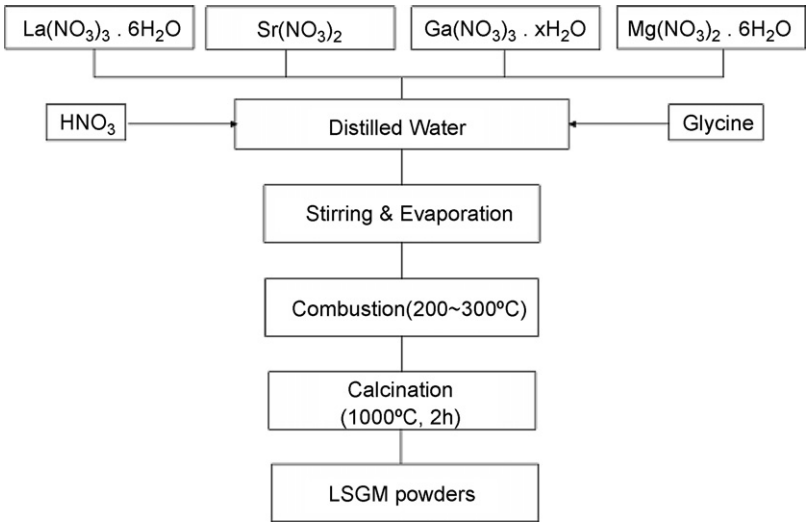

Fig. 1. The procedure for preparation of LSGM by glycine nitrate process.

the amount of Sr or Mg dopant was less than 20 at.%. Polymeric precursors for the LSGMs were synthesized using GNP and calcined at 1000 °C for 2 h. The procedure was as outlined in Fig. 1. In the process, $La(NO_3)_3{\cdot}6H_2O$, $Sr(NO_3)_2$, $Ga(NO_3)_3{\cdot}xH_2O$ and $Mg(NO_3)_2{\cdot}6H_2O$ were used as the starting materials together with glycine as the fuel. The calcined powders were put in a jar with ethyl alcohol and milled for 24 h using zirconia balls so that they could get released from agglomeration. Agglomeration usually leads to poor compaction of powders and eventually affects the sinterability of green compacts. The slurry was then dried in an oven. The resultant powder was crushed in a mortar, passed through a #120 sieve, compacted into a disc (Ø20 mm) or a rod (Ø6 mm), and sintered at 1400 °C for 4 h in air.

The XRD (X-ray diffraction) analysis (Rigaku Geigerflex DMAX-II A) was made with the LSGMs of four compositions in as-synthesized, as-calcined and as-sintered states to identify the phases and determine the particle sizes. The sintering temperature was varied from 1100 °C to 1500 °C with a fixed time of 4 h. The purpose of the analysis was two-fold. One was to determine the optimum sintering temperature and the other was to see whether or not there existed any second phases except the main LSGM phase because the existence of second phases in the specimen may affect its electrical conductivity.

The electrical conductivities of the LSGMs, which are considered with first priority among the requirements that an electrolyte should meet, were measured using an impedance analyzer (HP4192A) at various temperatures in the range of 550–800 °C and the composition with the maximum conductivity was determined from the result. Pt paste was painted on both sides of a disc specimen and fired at 900 °C for 3 h to form the electrodes necessary for the measurement. The specimen of the composition with the maximum conductivity was then characterized using field emission scanning electron microscopy (FE-SEM, Hitachi 6300) and thermomechanical analysis (TMA, Shimadzu 60H) to see if it fulfilled the other requirements. The relative density of the sinter was measured using the Archimedes method. A mixture of LSGM/LSM powders with a weight ratio of 1:1 was prepared for the experiment to examine the phase stability of the LSGM at the cathode side interface. Similar experiments were also conducted with a mixture of LSGM/NiO powders or LSGM/YSZ powders to examine the phase stability of the LSGM at the anode side interface. For uniform mixing, the powder mixture was wet-milled in a mortar using an agent of ethyl alcohol and pressed into a disc. The disc was heated at a temperature of 1400 °C for 4 h for sufficient reaction between the two materials and then crushed again in a mortar into powders for XRD analysis to examine whether or not there were any reaction products formed during heating.

3. Results and discussion

The XRD patterns of LSGM8282 and LSGM8291 for the as-sintered state are respectively shown in Figs. 2 and 3 together with those for the as-synthesized and as-calcined states. The XRD patterns were also obtained for the other two composi-

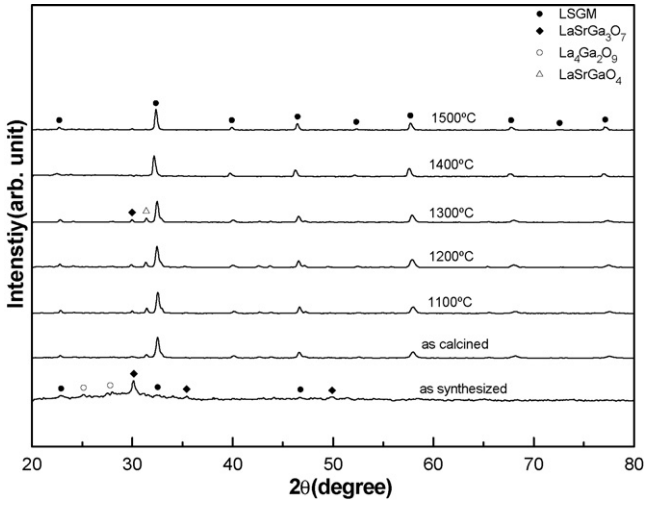

Fig. 2. XRD patterns of LSGM8282, as synthesized by the GNP, as calcined at 1000 °C for 2 h, and as sintered at various temperatures for 4 h.

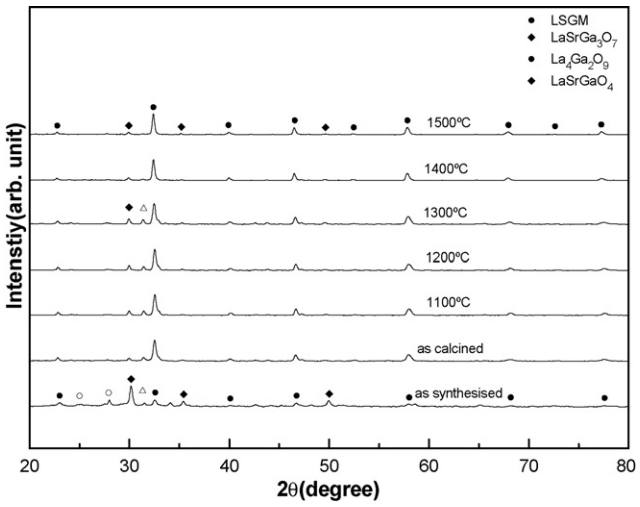

Fig. 3. XRD patterns of LSGM8291, as synthesized by GNP, as calcined at 1000 °C for 2 h, and as sintered at various temperatures for 4 h.

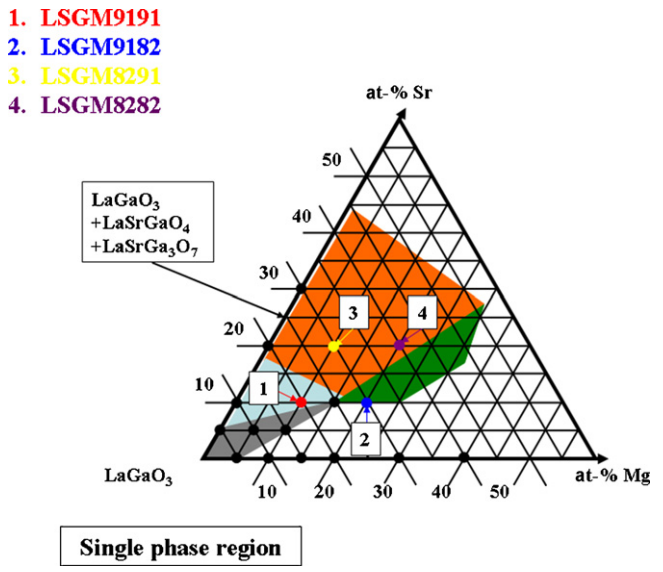

Fig. 4. Equilibrium phase diagram for a ternary $LaGaO_3$–Sr–Mg system [2].

tions, but are not shown here because they were almost identical to those for LSGM8282 in Fig. 2. It can be seen in Fig. 2 that the LSGM8282 consists of three phases of $LaSrGa_3O_7$, $La_4Ga_2O_9$ and LSGM in the as-synthesized state and so did the LSGM9191 and LSGM9182. The LSGM8291, however, contains the $LaSrGaO_4$ phase as well in addition to the above three phases as can be seen in Fig. 3. When calcined, the LSGM becomes the main phase, regardless of the composition, with some second phases like $LaSrGa_3O_7$ and $LaSrGaO_4$ as you can see also in figures.

The grain size of the calcined powder would be a very important parameter to influence on the sinterability of the green compacts since the powder in the as-calcined state was used for the compaction. Therefore, it was calculated from the (1 1 0) peak located at around 32.5° in figures using the Scherrer formula and Table 1 shows the values thus obtained for the four compositions. According to these results, the particle size of the LSGM powders shows almost no difference from composition to composition and is about 30 nm. Such a fine particle size would be expected to result in good sinterability.

The phase distribution in the as-calcined state remains in the as-sintered state until the sintering temperature reaches 1400 °C where the peaks for the above-mentioned second phases completely disappear except in the LSGM8291. In the case of LSGM8291, the peaks do not disappear completely, but much weakened. The explanation for this can be found in Fig. 4 where the equilibrium phase diagram for a ternary $LaGaO_3$–Sr–Mg system is given [3]. According to this diagram, the three compositions of LSGM8282, LSGM9191 and LSGM9182 are very close to a single-phase region, whereas, the composition of LSGM8291 is definitely far away from the single phase region. No difference was noticed in the XRD patterns when the sintering temperature was raised from 1400 °C to 1500 °C. Therefore, the sintering temperature was finally set at 1400 °C.

Fig. 5 shows the SEM images for the LSGMs of the four compositions. Regardless of the composition, grains are easily recognizable and there exist no pores, which would have been observed if the sintering process were incomplete. The values of the average grain size estimated from the images and of the relative density measured using the Archimedes method are summarized in Table 2. The grain size was ~3 μm for LSGM9191 and LSGM8291 and ~5 μm for LSGM9182 and LSGM8282. The reason for this difference in the grain size is not known yet. But, from the viewpoint of the grain boundaries as scattering centers for charge carriers, the LSGM9182 and LSGM8282 with relatively larger grain sizes (or smaller grain boundary areas) than the other two are expected to show higher ionic conductivities. The relative density values are very high ranging from 98.2% to 99.8%. Although expected once already from the SEM images, these results confirm that the LSGMs have been sintered to high densities. The sintering temperature of 1400 °C employed in this experiment is about 150 °C lower than that employed in other works, in which the LSGM was prepared by the solid state reaction [4]. One possible explanation as to why such a dense sinter could be formed at such a relatively low temperature may be given by the fine particle size

Table 1
Particle sizes for LSGMs of various compositions calcined at 1000 °C for 2 h

Composition	Particle size (nm)
LSGM9191	28.9
LSGM9182	29.6
LSGM8291	31.2
LSGM8282	28.2

Table 2
Average grain sizes and relative densities for LSGMs of various compositions sintered at 1400 °C for 4 h

Composition	Average grain size (μm)	Relative density (%)
LSGM9191	3.3	98.2
LSGM9182	5.5	99.3
LSGM8291	2.8	98.6
LSGM8282	4.9	99.8

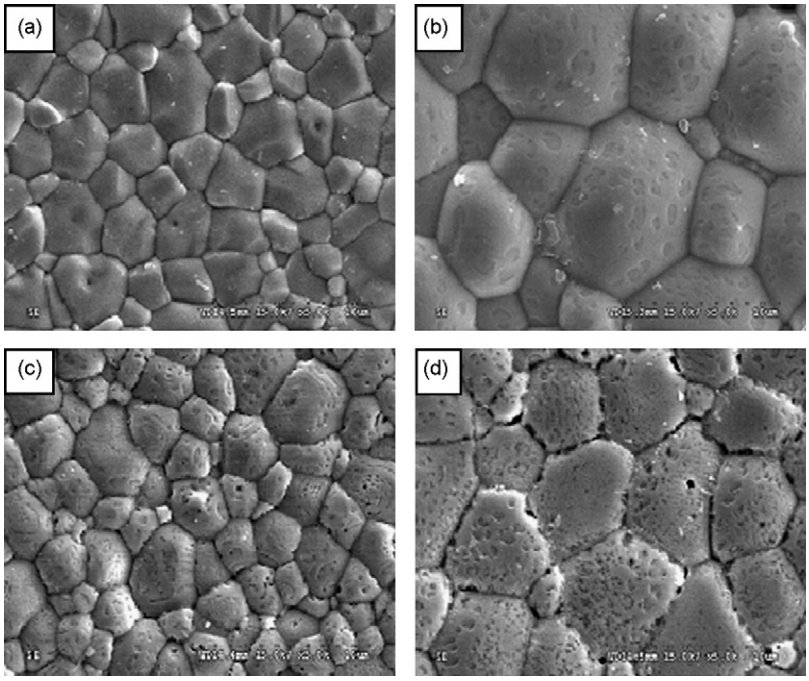

Fig. 5. SEM images for (a) LSGM9191, (b) LSGM9182, (c) LSGM8291 and (d) LSGM8282 compositions sintered at 1400 °C for 4 h.

mentioned above regarding Table 1. It can be considered quite advantageous that the electrolyte is able to be sintered into a dense film at such a low temperature when it has to be co-fired with the anode as in the case of the anode-supported cell.

The Arrhenius plot for the electrical conductivity of the LSGM9191, LSGM9182, LSGM8291 and LSGM8282 compositions is shown in Fig. 6 together with that of YSZ for comparison. It can be seen in this figure that the electrical conductivity is the lowest in LSGM9191, increases in the order of LSGM9191, LSGM8291, LSGM9182 and LSGM8282 and is the highest in LSGM8282. The ionic conductivity of $LaGaO_3$, which is itself a poor conductor, is known to increase to a certain extent as more Sr^{2+} ions are substituted for La^{3+} ions. From this, it can be predicted that LSGM8291 and LSGM8282 would have higher ionic conductivities than the other two compositions. However, as can be seen in the phase diagram (Fig. 4), the solubility limit of Sr^{2+} in $LaGaO_3$ increases as more Mg^{2+} ions are substituted for Ga^{3+} ions. Thus, the LSGM8291 with a relatively small amount of Mg^{2+} ions (or relatively low solubility limit of Sr^{2+} in $LaGaO_3$) is expected to contain significant amounts of second phases as already confirmed above by the XRD results. These second phases might have lowered somewhat the conductivity of LSGM8291. In the case of LSGM8282, the conductivity value was read as 0.105 S cm^{-1} at a temperature of 800 °C which is more than twice as high as ~0.045 S cm^{-1} for YSZ [5]. This value can be compared with 0.0606 S cm^{-1} [6] for LSGM82 (8.5)(1.5) prepared by GNP, 0.093 S cm^{-1} [7] for LSGM (8.5)(1.5)(8.5)(1.5) prepared by acrylamide polymerization and ~0.1 S cm^{-1} [8] for LSGM9191 prepared by solid-state reaction. As far as the ionic conductivity is concerned, the LSGM8282 is thus the greatest potential material at least among the four LSGMs that can replace YSZ electrolyte in IT-SOFCs.

Fig. 7 shows the result of thermomechanical analysis (TMA) obtained for the LSGM8282. For comparison it also shows the TMA results of YSZ and LSM. These two materials were selected for comparison because YSZ was the main ingredient of the anode and, among the two cathode materials of LSM and

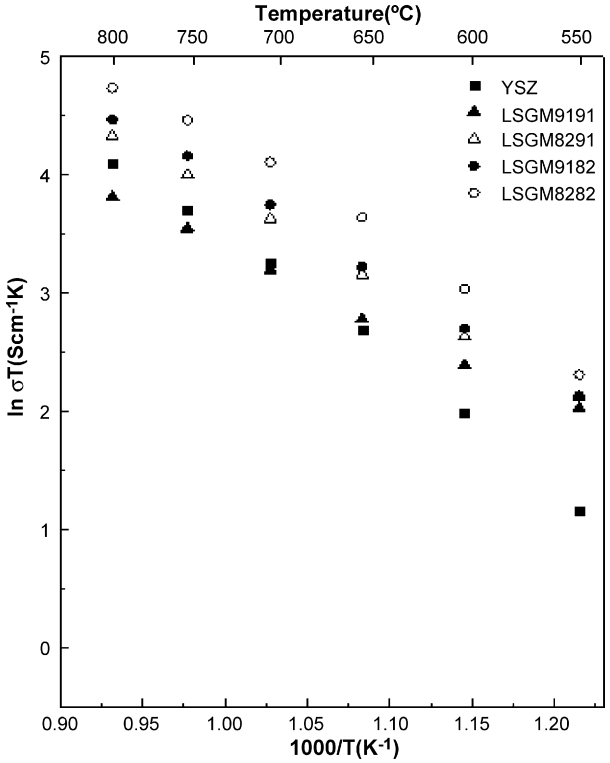

Fig. 6. Arrhenius plot for ionic conductivity of LSGM specimens sintered at 1400 °C for 4 h.

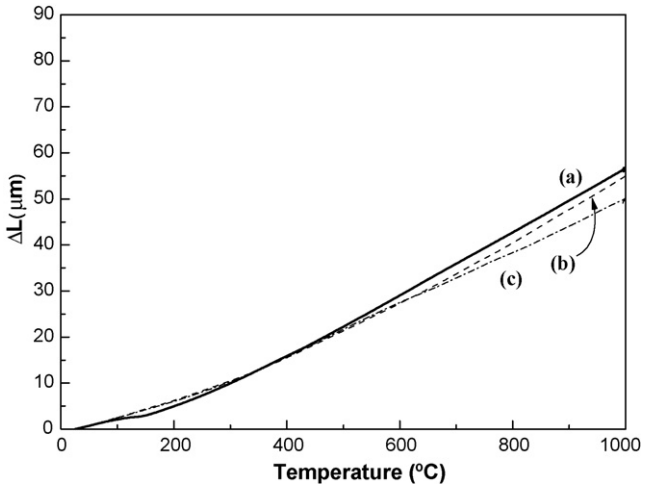

Fig. 7. Comparison of thermal expansion behaviors for (a) LSGM8282, (b) LSM and (c) YSZ.

LSCF, only the former was in direct contact with the electrolyte in the cell structure. The linear thermal expansion coefficient of LSGM8282 was estimated from the slope of the linear region from RT to 1000 °C as $12.1 \times 10^{-6}\ K^{-1}$. This value is very close to $11.7 \times 10^{-6}\ K^{-1}$ for LSM.

Fig. 8 shows the XRD patterns of the LSGM8282/LSM mixture obtained before and after heating at 1400 °C for 4 h. Since LSGM and LSM have the same crystal structure of perovskite, it is not easy to distinguish their XRD peaks. However, fortunately, the LSGM has a somewhat larger lattice parameter than the LSM and its XRD peaks are supposed to appear at relatively lower angles. No difference can be found between the XRD patterns before and after heating and no traces of peaks for the reaction products were observed anywhere in the pattern. The LSGM8282 is thus said to be fairly stable at the cathode side interface.

Figs. 9 and 10 show, respectively, the XRD patterns of the LSGM8282/NiO and LSGM8282/YSZ mixtures before and after heating at 1400 °C for 4 h. In both figures, the XRD pattern

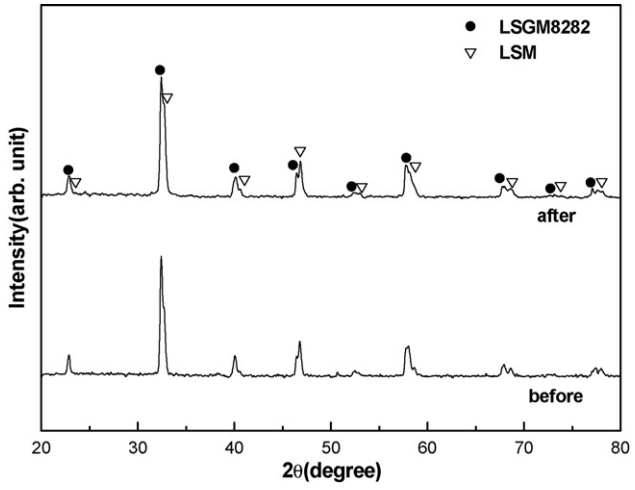

Fig. 8. Comparison of XRD patterns of an LSGM8282/LSM mixture before and after heating at 1400 °C for 4 h.

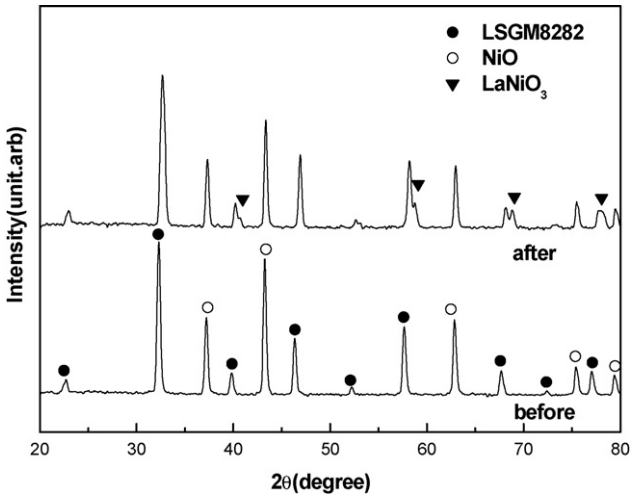

Fig. 9. Comparison of XRD patterns of an LSGM8282/NiO mixture before and after heating at 1400 °C for 4 h.

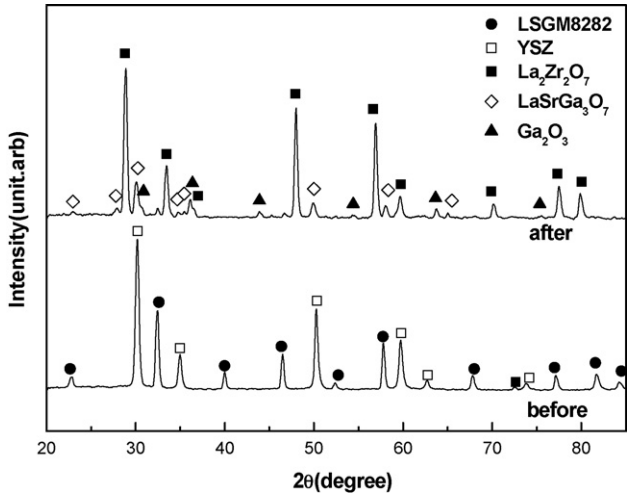

Fig. 10. Comparison of XRD patterns of an LSGM8282/YSZ mixture before and after heating at 1400 °C for 4 h.

after heating is definitely different from that before heating. The LSGM8282 must have reacted quite extensively with NiO or YSZ during heating to produce second phases such as $LaNiO_3$ in the former case or $La_2Zr_2O_7$, $LaSrGa_3O_7$ and Ga_2O_3 in the latter case. It is thus evident that the LSGM8282 is not stable at all at the anode side interface and some kind of buffer layer has to be used to prevent from direct reaction of LSGM8282 and anode materials.

4. Conclusions

LSGM ($La_{1-x}Sr_xGa_{1-y}Mg_yO_{3-\delta}$) powders of four different compositions (x, $y = 0.1$ or 0.2) were synthesized using the GNP, compacted into a disc or a rod and sintered at 1400 °C for 4 h in air. The XRD patterns show that the sinters of LSGM9191, LSGM9182 and LSGM8282 consisted of a single LSGM phase. The sinter of LSGM8291, however, contained the second phases of $LaSrGa_3O_7$ and $LaSrGaO_4$ as well in addition to the main LSGM phase. The electrical conductivity of LSGM8282 at

800 °C was 0.105 S cm^{-1} which turned out to be the highest among those of the four LSGMs and more than twice as high as that of YSZ (∼0.045 S cm^{-1}). Also, the linear thermal expansion coefficient of LSGM8282 was 12.1×10^{-6} K^{-1}, which is very close to that of LSM (11.7×10^{-6} K^{-1}), one of the cathode materials. Therefore, the LSGM8282 can be a strong candidate to replace YSZ as the electrolyte in IT-SOFCs when used with a buffer layer to prevent from direct reaction of LSGM and Ni–YSZ.

Acknowledgement

This study was financially supported by the Korea Institute of Energy Research.

References

[1] R. Song, E. Kim, D.R. Shin, H. Yokokawa, in: S.C. Singhal, M. Dokiya (Eds.), Proceedings of the 6th International Symposium on Solid Oxide Fuel Cells, Electrochemical Society, Pennington, USA, 1999, p. 845.
[2] L.A. Chick, L.R. Pederson, G.D. Maupin, Mater. Lett. 10 (1990) 6.
[3] P. Majewski, M. Rozumek, F. Aldinger, J. Alloys Comp. 239 (2001) 253.
[4] K.Q. Huang, M. Feng, B.J. Goodenough, J. Am. Ceram. Soc. 79 (1996) 1100.
[5] Y. Arachi, H. Sakai, O. Yamamoto, Y. Takeda, N. Imanishi, Solid State Ionics 121 (1999) 133.
[6] L. Cong, T. He, Y. Ji, P. Guan, Y. Huang, W. Su, J. Alloys Comp. 348 (2003) 325.
[7] N. Liu, Y. Yuan, P. Majewski, F. Aldinger, Mater. Res. Bull. 41 (2005) 461.
[8] T. Ishihara, H. Matsuda, Y. Takita, J. Am. Chem. Soc. 116 (1994) 3801.